INTERNATIONAL JOURNAL OF OPTIMIZATION IN CIVIL ENGINEERING
Int. J. Optim. Civil Eng., 2025; 15(2):297-316

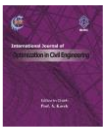

MULTI-MATERIAL TOPOLOGY OPTIMIZATION OF STRUCTURES BY USING THE METHOD OF MOVING ASYMPTOTES

Kh. Soleymanian and S. M. Tavakkoli[*, †]
Civil Engineering Department, Shahrood University of Technology, P.O. Box 3619995161, Shahrood, Iran

[DOI: 10.22068/ijoce.2025.15.2.639]

ABSTRACT

This study aims to deal with multi-material topology optimization problems by using the Methods of Moving Asymptotes (MMA) method. The optimization problem is to minimize the strain energy while a certain amount of material is used. Several types of structures, including plane, plate and shell structures, are considered and optimal materials distribution is investigated. To parametrize the topology optimization problem, the Solid Isotropic Material with Penalization (SIMP) method is utilized. Analytical sensitivity analysis is performed to obtain the derivatives of the objective function and volume constraints with respect to the design variables. Two types of material with different modulus of elasticities are considered and, therefore, each element has two design variables. The first design variable represents the presence or absence of material in an element, while the second design variable determines the type of material assigned to the element. In order to analyze the structures required during the optimization process, the ABAQUS software is employed. To integrate the topology optimization procedure with ABAQUS model, a Python script is developed. The obtained results demonstrate the performance of the proposed method in generating reasonable and effective topologies.

Keywords: Multi-material topology optimization, SIMP, Method of moving asymptotes, Strain energy minimization, plates, Shell structures.

Received: 11 May 2025; Accepted: 9 July 2025

1. INTRODUCTION

Optimization refers to determining the best possible outcome or result for a system while simultaneously satisfying certain constraints and limitations. Structural engineering design

[*]Corresponding author: Civil Engineering Department, Shahrood University of Technology, P.O. Box 3619995161, Shahrood, Iran
[†]E-mail address: mtavakkoli@shahroodut.ac.ir (S. M. Tavakkoli)

can be divided into three main stages. In the first stage, the structural form and layout are determined based on the design space. The second stage involves defining the shape of the structure and the geometric characteristics of its boundaries. The third stage pertains to the detailed design of structural elements. This categorization has, respectively, led to the development of three corresponding structural optimization methods: topology optimization, shape optimization, and size optimization.

In 1988, Bendsøe and Kikuchi [1] introduced the concept of topology optimization by using the homogenization method, however, the foundation of this method goes back to the minimum weight structures that developed by Michell [2] in 1904. Bendsøe [3] proposed the use of penalization for isotropic materials for the first time in 1989. By 1992, Rozvany and colleagues [4] developed the Solid Isotropic Material with Penalization (SIMP) method, incorporating penalized intermediate design variables to achieve a black-and-white model. Over the years, various topology optimization (TO) methods have been developed, including the optimality criteria methods [5-7], Evolutionary Structural Optimization (ESO) [8, 9], Bidirectional Evolutionary Structural Optimization (BESO) [10], the Level-Set Methods (LSM) [11-17] and several metaheuristic approaches such as the ant colony method, etc. for continuum and skeleton structures [18-27]. In this study, the Method of Moving Asymptotes (MMA), which has been proven to be among the most effective methods for solving topology optimization problems, is utilized as the optimization engine. This method was introduced by Svanberg in 1987 [28] and has vastly been used in structural optimization [29-33].

Multi-material topology optimization primarily aims to achieve optimal performance through the efficient distribution of different materials [34] or realize purposes that may be difficult to be attained by single-material structures [35]. Zuo and Saitou [36] proposed a multi-material interpolation scheme based on the Solid Isotropic Material with Penalization (SIMP) method to solve multi-material topology optimization problems using the Optimality Criteria (OC) algorithm. Su Yun and Kie Youn [37] developed a multi-material topology optimization approach with the objective of maximizing dissipated energy, aiming to design viscoelastic and structural systems that exhibit both high damping and desirable stiffness. In light of recent advancements in 3D printing technology, Li et al. [38] proposed a novel multi-material topology optimization approach for designing 3D-printable concrete structures. Zhang et al. [39], noting that most studies on multi-material topology optimization have focused on continuous structures under linear material behavior, conducted a study on topology optimization of truss structures by considering nonlinear material behavior. Li and Kim [40] addressed the multi-material optimization problem by introducing a method based on element-wise density to minimize strain energy while satisfying volume constraints. Chandrasekhar and Suresh [41] solved the multi-material topology optimization problem through the implementation of neural networks. Feng and Yamada [42], pointing out that existing research often assumes multi-material structures are assembled using welding or adhesives which do not support disassembly and are unsuitable for manufacturing, thus proposed an innovative approach for generating interlocking connections in multi-material topology optimization, enabling easy assembly and disassembly. Jeong et al. [43] introduced a novel method for multi-material topology optimization based on Physics-Informed Neural Networks (PINNs), capable of solving complex and nonlinear problems. Duan et al. [44] proposed a multi-material topology optimization approach for structural design decision-making, which identifies optimal topologies that enhance load-bearing capacity and reduce

[DOI: 10.22068/ijoce.2025.15.2.639]

costs by considering both strain energy and material expenses. Yang et al. [45] presents a multi-material topology optimization method for designing additive manufactured thin-walled structures with optimized lattice and stiffener layouts. Numerical and experimental results demonstrate that the proposed approach significantly improves structural performance compared to conventional designs. Zhao in reference [46] presented a multi-material topology optimization method for identifying strut and tie model in deep reinforced concrete beams. Li et al. [47] proposed a multi-material topology optimization strategy tailored for the architectural design of structures. Chu et al. [48] introduced a two-stage filtering approach to characterize multi-material structures for topology optimization. Banh and Lee [49] developed a multi-material topology optimization method for continuous structures based on crack pattern evolution, aiming to generate optimal topologies and material distributions to prevent crack propagation. Jahangiri et al. [50] investigated the multi-material topology optimization of steel shear walls using the level set method, taking into account the effects of stiffeners and architectural openings. It was observed that multi-material shear walls reduced the strain energy thereby decreasing lateral displacements. Zhengtong et al. [51] applied an enhanced version of the Particle Swarm Optimization (PSO) algorithm to the multi-material topology optimization problem. Kaveh et al. [52] applied an improved firefly algorithm to optimize the topology and connectivity of multi-material truss structures. One of the recently developed meta-heuristic algorithms is the Black Hole Mechanics Optimization (BHMO) algorithm. Salmanpour et al. [53] conducted a study on multi-material size optimization of transmission tower trusses using the Black Hole Mechanics Optimization (BHMO) algorithm.

Topology optimization has demonstrated its capability in generating optimal designs across various fields of engineering. However, the widespread application of many modern methods in academic and industrial settings has been limited due to implementation challenges within commercial software environments. In this study, the topology optimization problem is implemented using the Python programming language, while structural analysis throughout the optimization process is carried out using the finite element software, ABAQUS.

[DOI: 10.22068/ijoce.2025.15.2.639]

2. PARAMETERIZATION OF THE OPTIMIZATION PROBLEM

Based on the Solid Isotropic Material with Penalization (SIMP) method, the interpolation function for the multi-material modulus of elasticity can be expressed as [40]:

$$\begin{aligned} E_{ijkl}(\rho^{1,M}) &= (\rho^{1})^{P} E_{ijkl}^{1,M} = (\rho^{1})^{P}\left[(\rho^{2})^{P} E_{ijkl}^{1} + \left[(1-(\rho^{2})^{P}\right] E_{ijkl}^{2,M}\right]... \\ \textit{where} \quad & E_{ijkl}^{m,M} = (\rho^{m+1})^{P} E_{ijkl}^{m} + \left[1-(\rho^{m+1})^{P}\right] E_{ijkl}^{m+1,M} \\ \textit{and} \quad & E_{ijkl}^{M,M} = E_{ijkl}^{M},\ m = 1,2...,M \end{aligned} \tag{1}$$

where $E_{ijkl}(\rho^{1,M})$ is the index representation of the interpolated elasticity tensor, $E_{ijkl}^{m,M}$ is the recursive representation associated with m base materials, and P is the penalization factor generally assumed to be equal to 3 in the numerical simulation.

In this paper, the material interpolation function for a two-material interpolation is written as follows:

$$E_{ijkl}(\rho^1,\rho^2)=\left(\rho^1\right)^P\left[(\rho^2)^P E^1_{ijkl}+\left[1-(\rho^2)^P\right]E^2_{ijkl}\right] \tag{2}$$

where E_{ijkl} denotes the elasticity tensor of each finite element. ρ^1 is the first design variable indicating the presence or absence of material in an element, and ρ^2 is the second design variable that determines the type of material assigned to the element. Here E^1_{ijkl}, E^2_{ijkl} denote the elasticity tensors of the first and second materials, respectively. In the examples of this study, the first material is assumed to be the stiffer one. Accordingly, two design variables are necessary to represent the three-phase material model, two solid and one void materials. In general, the extension of the SIMP approach to an *m*-phase material model demands $(m-1)$ design variables per finite element.

3. METHOD OF MOVING ASYMPTOTES

The MMA is a gradient based nonlinear programming algorithm that is widely applied to structural optimization problems. This method employs an iterative scheme, wherein each step constructs a series of strictly convex approximating subproblems. At each iteration point, subproblems are solved using the dual method, and their solutions are utilized as the next iteration point. This iterative process continues until convergence is achieved. In this method, the approximation function for each $j=0,...,m$ around the iteration point $x^{(k)}$, where x is the vector of design variables with n components and k is iteration counter is defined as follows [28]:

$$g_j^{(k)}(x)\approx r_j^{(k)}+\sum_{i=1}^{n}\left(\frac{p_{ji}^{(k)}}{U_i^{(k)}-x_i}+\frac{q_{ji}^{(k)}}{x_i-L_i^{(k)}}\right) \tag{3}$$

The values of $r_j^{(k)}$, $p_{ji}^{(k)}$ and q_{ji}^{k} are selected as follows:

$$\begin{aligned}
r_j^{(k)} &= g_j(x^{(k)})-\sum_{i=1}^{n}\left(\frac{p_{ji}^{(k)}}{U_i^{(k)}-x_i^{(k)}}+\frac{q_{ji}^{(k)}}{x_i^{(k)}-L_i^{(k)}}\right)\\
p_{ji}^{(k)} &= (U_i^{(k)}-x_i^{(k)})^2\times\frac{\partial g_j}{\partial x_i} \qquad if \quad \frac{\partial g_j}{\partial x_i}>0\\
p_{ji}^{(k)} &= 0 \qquad if \quad \frac{\partial g_j}{\partial x_i}\le 0\\
q_{ji}^{(k)} &= 0 \qquad if \quad \frac{\partial g_j}{\partial x_i}\ge 0\\
q_{ji}^{(k)} &= -(x_i^{(k)}-L_i^{(k)})^2\times\frac{\partial g_j}{\partial x_i} \qquad if \quad \frac{\partial g_j}{\partial x_i}<0
\end{aligned} \tag{4}$$

[DOI: 10.22068/ijoce.2025.15.2.639]

The positive values $L_i^{(k)}$ and $U_i^{(k)}$ serve as bounding limits within which the approximation function is capable of generating reasonable solutions for the optimization problem. The values of these parameters, which are considered vertical asymptotes for the approximation function, must be updated in each iteration.

To solve the approximate subproblem using the dual method, the Lagrangian function must first be constructed and then minimized with respect to the design variables. By substituting the obtained minimum value into the Lagrangian function, which also depends on the Lagrange multipliers, this function must then be maximized with respect to the Lagrange multipliers. The value obtained in the final step represents the optimal point of the approximate subproblem [28]. To obtain the approximate formulation of the optimization problem, it is necessary to compute the derivatives of the objective and constraint functions with respect to the design variables as input data.

4. FORMULATION OF THE TOPOLOGY OPTIMIZATION PROBLEM CONSIDERING TWO MATERIALS

The topology optimization problem for minimizing strain energy is expressed as follows:

$$\begin{aligned} &\min C(\rho^1,\rho^2)=\frac{1}{2}U^T KU \\ &\textit{subject to}: \quad KU=F \\ &\qquad \sum_{i=1}^{N}\rho_i^1 v_i \le V_{Total-\max} \\ &\qquad \sum_{i=1}^{N}\rho_i^1\rho_i^2 v_i \le V_{1-\max} \\ &\qquad 0<\rho_{\min}\le\rho_i^1\le 1,\ \ i=1,2,...,N \\ &\qquad 0\le\rho_i^2\le 1, \qquad\quad i=1,2,...,N \end{aligned} \tag{5}$$

where C denotes the strain energy, which serves as the objective function; ρ^1 is the first design variable indicating the presence or absence of material in each finite element; and ρ^2 is the second design variable specifying the type of material assigned to each element. The topology optimization problem is subject to two volume constraints: $V_{total-\max}$, which represents the total allowable volume of both materials combined, and $V_{1-\max}$, which limits the volume of the first material. Additionally, v_i denotes the volume of the i-th element. K is the global stiffness matrix, U is the nodal displacement vector, F is the external force vector, and N is the number of elements within the design domain.

[DOI: 10.22068/ijoce.2025.15.2.639]

5. SENSITIVITY ANALYSIS

In optimization problems, this concept refers to assessing the sensitivity of the objective function with respect to each design variable, which essentially involves computing the derivative of the objective function with respect to that variable. In general, sensitivity analysis methods can be categorized into three main types: numerical, semi-analytical, and analytical approaches. In numerical methods, the derivatives of the objective and constraint functions are obtained using various numerical techniques, such as finite difference schemes. Semi-analytical methods involve a combination of analytical and numerical procedures to compute the required derivatives. In analytical methods, which are employed in this study, the derivatives are explicitly derived with respect to the design variables of the problem.

In structural topology optimization problems, the number of finite elements and consequently the number of design variables is typically very large. Therefore, the use of the adjoint variable method for sensitivity analysis, particularly through the computation of the adjoint variable λ, is highly suitable and computationally efficient. Sensitivity analysis using the adjoint method, in conjunction with the Solid Isotropic Material with Penalization (SIMP) approach, is defined by the following expression:

$$\begin{aligned}\frac{\partial C}{\partial \rho_i^j} &= \frac{\partial (F^T U - \lambda^T (KU - F))}{\partial \rho_i^j} = (F^T - \lambda^T K)\frac{\partial U}{\partial \rho_i^j} - \lambda^T \frac{\partial K}{\partial \rho_i^j} U \\ &= -\lambda^T \frac{\partial K}{\partial \rho_i^j} U \quad when\ F^T = \lambda^T K \Rightarrow\ \lambda = U\ \text{(self adjoint)} \\ \frac{\partial C}{\partial \rho_i^j} &= -U^T \frac{\partial K}{\partial \rho_i^j} U \quad i = 1,2,...,N;\ j = 1,2\end{aligned} \tag{6}$$

where F denotes the external force vector, K is the global stiffness matrix, U is the nodal displacement vector, and N represents the number of elements.

Similarly, the derivative of the objective function with respect to the first design variable is computed as follows [9]:

$$\begin{aligned}\frac{\partial C}{\partial \rho_i^1} &= -U^T \frac{\partial K}{\partial \rho_i^1} U = -u_i^T \frac{\partial k_i}{\partial \rho_i^1} u_i = -P(\rho_i^1)^{P-1}\left[(\rho_i^2)^P u_i^T k_i^1 u_i + (1-(\rho_i^2)^P) u_i^T k_i^2 u_i\right] \\ &= -\frac{P}{\rho_i^1}(\rho_i^1)^P\left[(\rho_i^2)^P u_i^T k_i^1 u_i + (1-(\rho_i^2)^P) u_i^T k_i^2 u_i\right] = -\frac{P}{\rho_i^1} u_i^T k_i u_i \\ &= -\frac{P}{\rho_i^1}(2StrainE_i)\end{aligned} \tag{7}$$

where k_i represents the stiffness matrix of the i-th element, k_i^1 is the element stiffness matrix computed using the elastic modulus of the first material, and k_i^2 is the element stiffness matrix computed using the elastic modulus of the second material. The strain energy of the i-th element is obtained from the following relation:

[DOI: 10.22068/ijoce.2025.15.2.639]

$$StrainE_i = \frac{1}{2} u_i^T k_i u_i \tag{8}$$

To compute the derivative of the objective function with respect to the second design variable, the following expression can be formulated:

$$\begin{aligned}
\frac{\partial C}{\partial \rho_i^2} &= -U^T \frac{\partial K}{\partial \rho_i^2} U = -u_i^T \frac{\partial k_i}{\partial \rho_i^2} u_i = -P(\rho_i^1)^P \left[(\rho_i^2)^{P-1} u_i^T k_i^1 u_i - (\rho_i^2)^{P-1} u_i^T k_i^2 u_i \right] \\
&= -\frac{P}{\rho_i^2} (\rho_i^1)^P \left[(\rho_i^2)^P u_i^T k_i^1 u_i - (\rho_i^2)^P u_i^T k_i^2 u_i \right] \\
&= -\frac{P}{\rho_i^2} (\rho_i^1)^P \left[(\rho_i^2)^P u_i^T k_i^1 u_i + (1-(\rho_i^2)^P) u_i^T k_i^2 u_i - u_i^T k_i^2 u_i \right] \\
&= -\frac{P}{\rho_i^2} \left[2StrainE_i - (\rho_i^1)^P u_i^T k_i^2 u_i \right]
\end{aligned} \tag{9}$$

In linear topology optimization, the term $(\rho_i^1)^P u_i^T k_i^2 u_i$ is defined as the pseudo strain energy [40], that can be written as follows:

$$StrainEC_i = (\rho_i^1)^P \frac{1}{2} u_i^T k_i^2 u_i = \frac{E^2}{(\rho_i^2)^P E^1 + (1-(\rho_i^2)^P) E^2} StrainE_i \tag{10}$$

Finally, the derivative of the objective function with respect to the second design variable is defined by the following relation:

$$\frac{\partial C}{\partial \rho_i^2} = -\frac{P}{\rho_i^2} \left[2StrainE_i - \frac{2E^2}{(\rho_i^2)^P E^1 + (1-(\rho_i^2)^P) E^2} StrainE_i \right] \tag{11}$$

6. OPTIMIZATION FRAMEWORK

The two-material topology optimization process can be explained by the flowchart depicted in Figure 1, which shows steps outlined as follows:

1. First step is the definition of design domain to be optimized.
2. The design domain is discretized into square quadratic finite element, at the end of this step, the ABAQUS model is prepared.
3. Execute a linear static finite element analysis of the structure.
4. Determine the strain energy of each element.
5. In this step an analytical sensitivity analysis is implemented based on Equations (7) and (11).
6. The Method of Moving Asymptotes (MMA) is employed to iteratively update the design variables.

[DOI: 10.22068/ijoce.2025.15.2.639]

7. The iterative procedure is repeated for the updates of the design variables until the minimization algorithm reaches convergence. Convergence is achieved when the objective function has not changed more than 0.1% over the last 10 iterations.

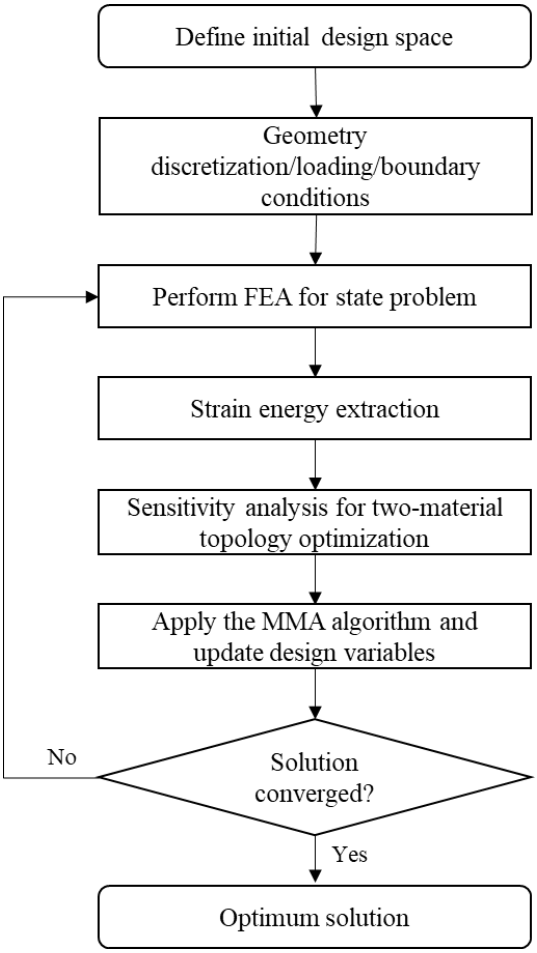

Figure 1: Flowchart of the proposed multi-material topology optimization

7. NUMERICAL EXAMPLES

7.1. Example 1

In this example, a fixed-end beam, as shown in Figure 2, is considered. The external force F in Figure 2 is equal to 5000 kgf in all cases. The design domain is discretized by 80×20 quadratic finite element. Topology optimization of two materials is investigated in which modulus of elasticities for material 1 and material 2 are 2×10^6 kg/cm^2 and 2×10^4 kg/cm^2, respectively. In order to investigate the effect of material volume fraction on the distribution of materials and performance of optimized structures, the problem is solved in four states with different volume fraction where the maximum total allowable volume of both materials are the same. The four volume fractions listed in Table 1.

[DOI: 10.22068/ijoce.2025.15.2.639]

The layout comparison of the four optimum solution for two-material topology optimization are shown in Figure 3. As evidenced by the results, Material 1 that consider as the stiffer material is allocated to regions of heightened stress concentration, such as near support boundaries and load application points. Conversely, the more compliant material is deployed in low stress zones. The convergence history of objective function and volume fractions of the solved problems is illustrated in Figure 4. As per Figure 4 it can be observed that as the amount of the stiffer material increases, the strain energy of the structure decreases, leading to an overall increase in stiffness.

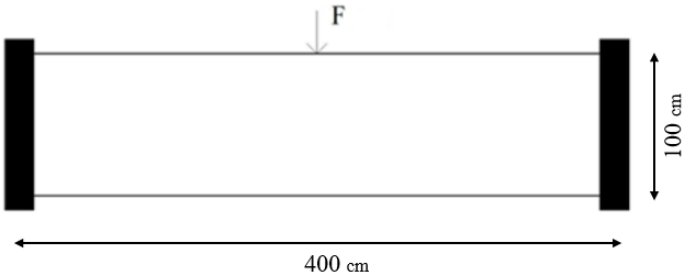

Figure 2: Geometry and boundary conditions

Table 1. Volume fraction constraints for the fixed-end problem

Case no.	Total material $(\frac{V_{\text{total-max}}}{V_{\text{design space}}})\%$	Material 1 $(\frac{V_1}{V_{\text{design space}}})\%$	Material 2 $(\frac{V_{\text{total-max}}-V_1}{V_{\text{design space}}})\%$
1	50	10	40
2	50	20	30
3	50	30	20
4	50	40	10

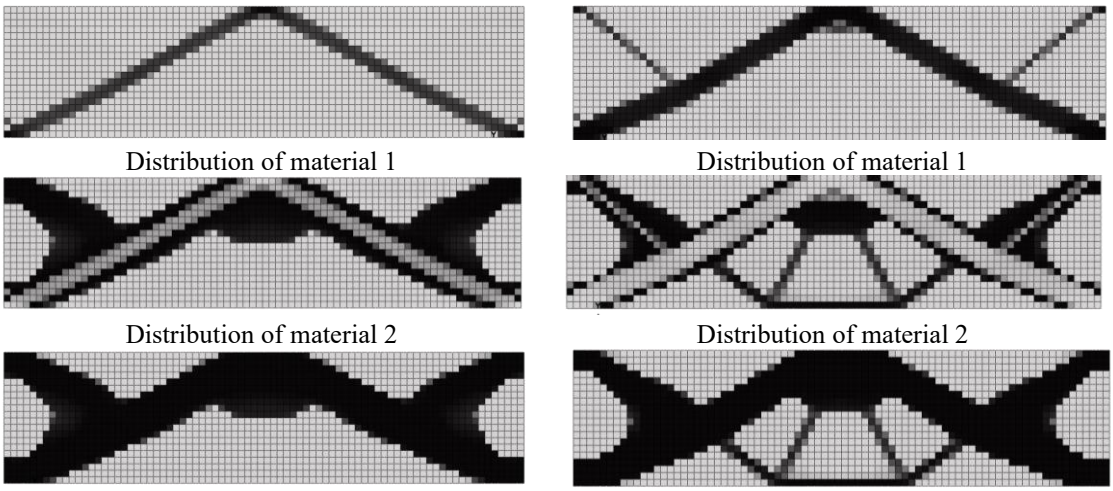

[DOI: 10.22068/ijoce.2025.15.2.639]

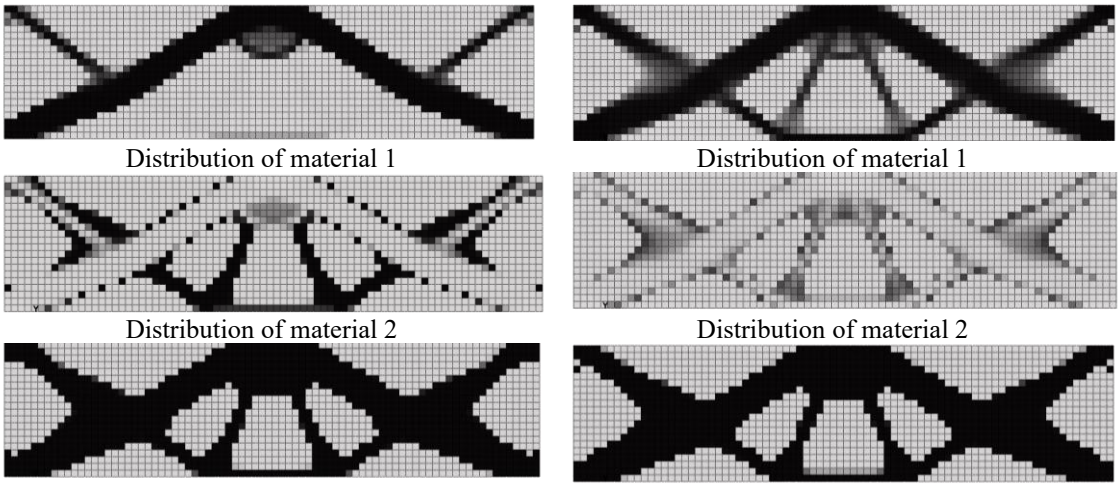

Figure 3: Optimum topology results of the end fixed beam. (a) Case 1; (b) Case 2; (c) Case 3; (d) Case 4

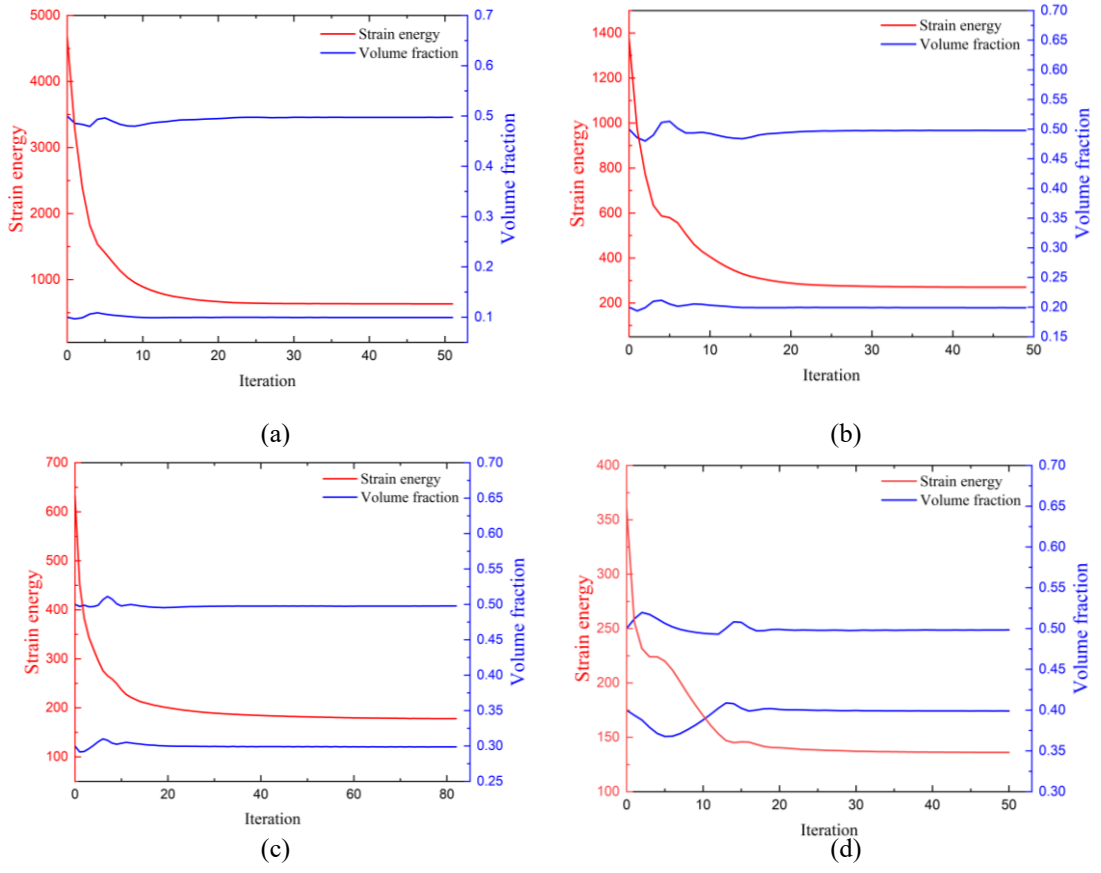

Figure 4: History of objective function and volume of end fixed beam. (a) Case 1; (b) Case 2; (c) Case 3; (d) Case 4

[DOI: 10.22068/ijoce.2025.15.2.639]

7.2. Example 2

A simple seated beam is studied in this example as depict in Figure 5. The design domain is meshed by 80×20 quadratic finite elements. The external force F in Figure 5 is equal to 5000 kgf in all cases. In order to investigate the effect of modulus of elasticities of material 2 on the distribution of materials and performance of optimized structures, the problem is solved in three states with different modulus of elasticities for material 2 which are shown in table 2. Maximum allowable volume of material 1 and maximum total allowable materials volume, are the same in these three states. The topology comparison of the three optimum solution for two-material topology optimization and convergence history of objective function and volume fractions are shown in Figures 6 and 7, respectively. As evidenced by the results, the distribution of materials 1 and 2 and the overall topology are independent of the value of the elastic modulus of the materials.

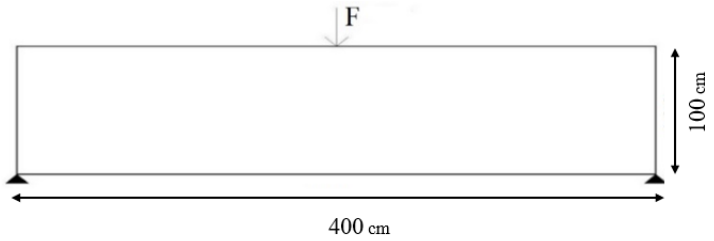

Figure 5. Geometry and boundary conditions.

Table 2: Volume fractions and modulus of elasticities of material 2.

Case no.	Total material $(\frac{V_{\text{total-max}}}{V_{\text{design space}}})\%$	Material 1 $(\frac{V_1}{V_{\text{design space}}})\%$	Material 2 $(\frac{V_{\text{total-max}}-V_1}{V_{\text{design space}}})\%$	Modulus of elasticities kg/cm^2
1				$E^2 = 2 \times 10^2$
2	50	30	20	$E^2 = 2 \times 10^3$
3				$E^2 = 2 \times 10^4$

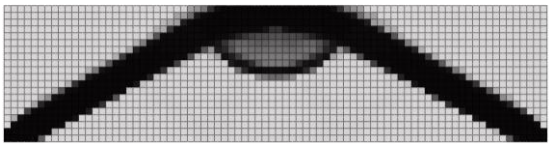

Distribution of material 1

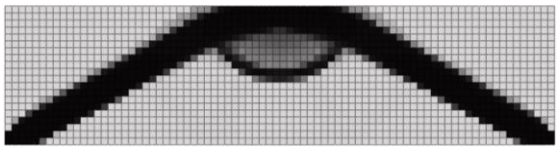

Distribution of material 1

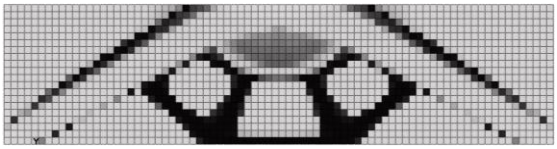

Distribution of material 2

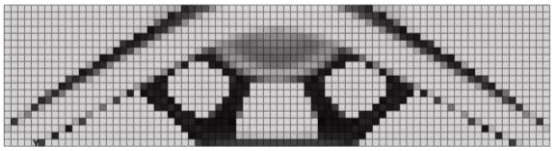

Distribution of material 2

[DOI: 10.22068/ijoce.2025.15.2.639]

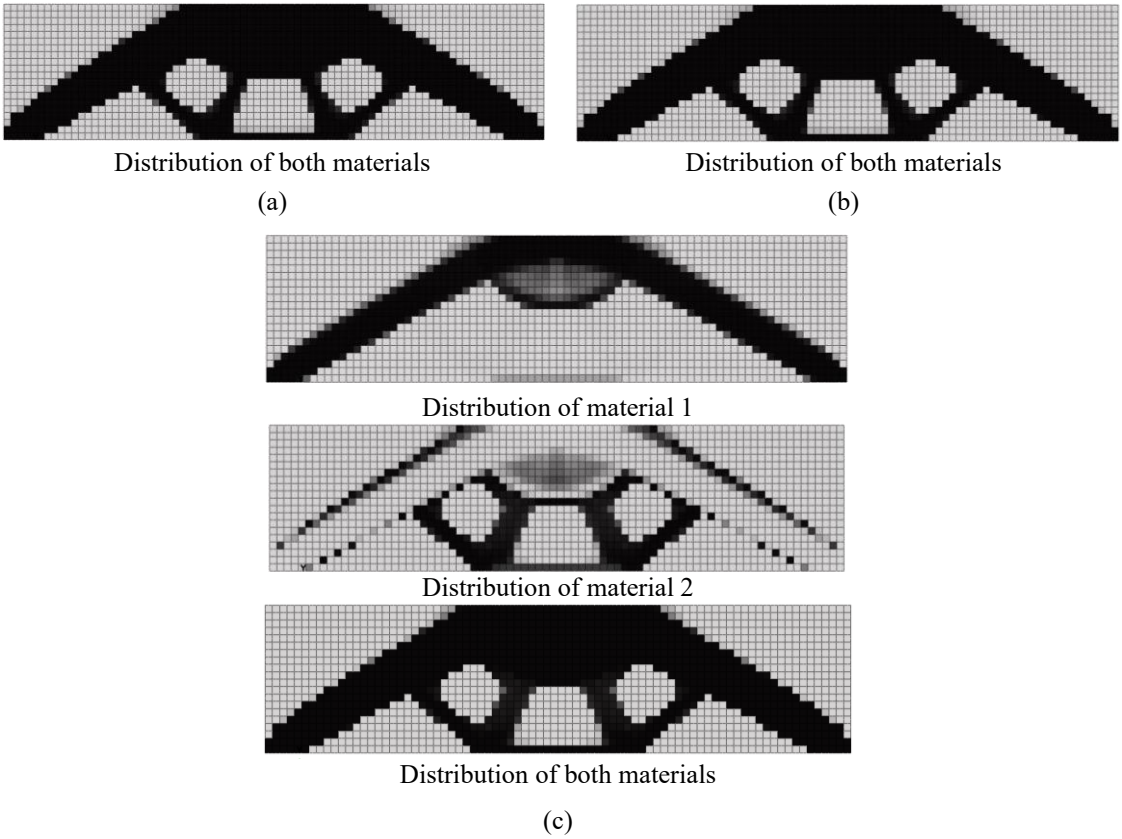

Figure 6: Optimum topology results of simple seated beam. (a) Case 1; (b) Case 2; (c) Case 3

7.3. Example 3

This example considers a plate structure with simply supported boundary condition at all four corners as depicted in Figure 8. This example is solved with two different mesh discretizations: in the first case, the design domain consists of 1000 quadratic finite element, and in the second case, it is discretized into 4000 quadratic finite element. The external force F in Figure 8 is equal to 1000 kgf in two cases. Topology optimization of two materials are investigated in which modulus of elasticities for material 1 and material 2 are 2×10^6 kg/cm^2 and 2×10^4 kg/cm^2, respectively. The volume fraction that used in this example is listed in table 3, and the topology comparison of the two optimum solution for two-material topology optimization and convergence history of objective function and volume fractions are shown in Figures 9 and 10, respectively. The results show that stiffer material is placed where the stress is higher. There is also a slight effect from the mesh, which is common in topology optimization problems.

[DOI: 10.22068/ijoce.2025.15.2.639]

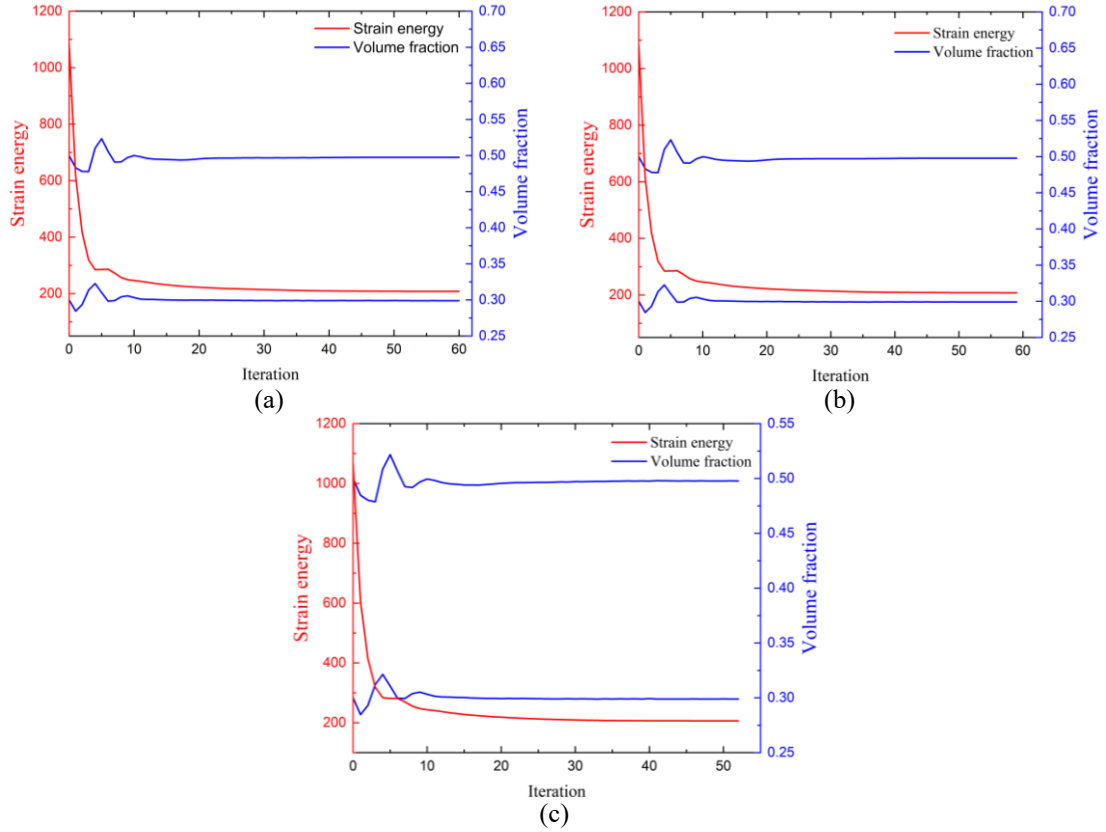

Figure 7: History of objective function and volume fraction of simple seated beam. (a) Case 1; (b) Case 2; (c) Case 3

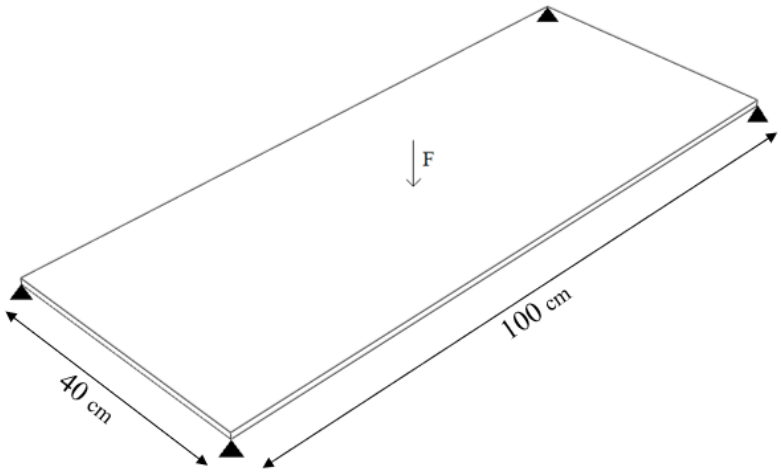

Figure 8: Geometry and boundary conditions

[DOI: 10.22068/ijoce.2025.15.2.639]

Table 3: Volume fraction constraints for plate structure

Case no.	Design domain elements	Total material $(\frac{V_{\text{total-max}}}{V_{\text{design space}}})\%$	Material 1 $(\frac{V_1}{V_{\text{design space}}})\%$	Material 2 $(\frac{V_{\text{total-max}}-V_1}{V_{\text{design space}}})\%$
1	20×50	50	20	30
2	40×100			

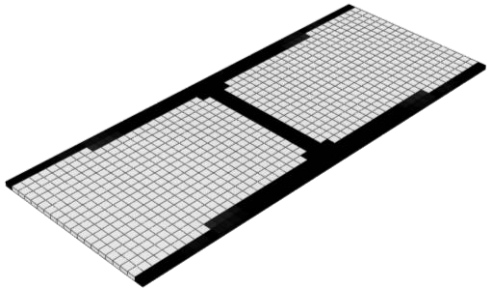

Distribution of material 1

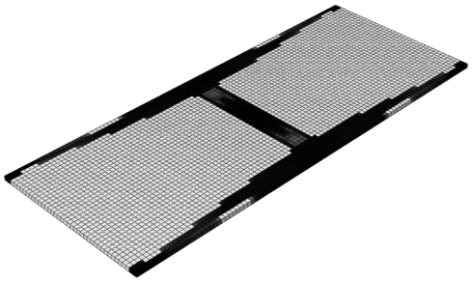

Distribution of material 1

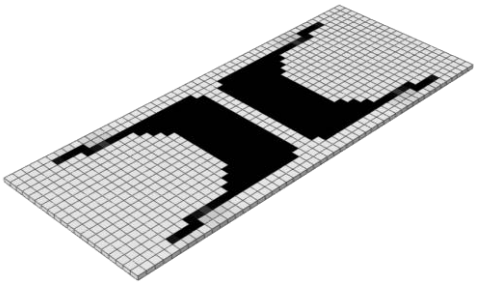

Distribution of material 2

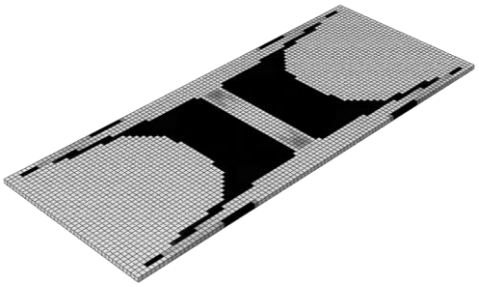

Distribution of material 2

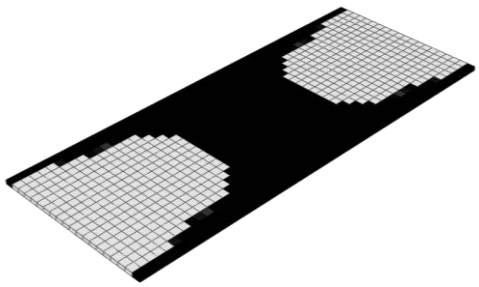

Distribution of both materials

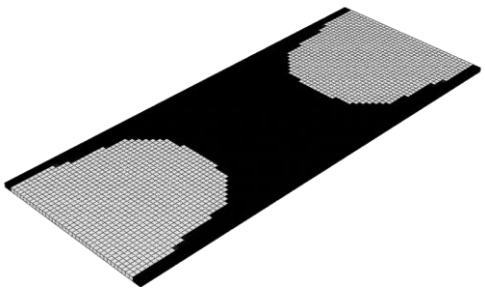

Distribution of both materials

(a) (b)

Figure 9: Optimum topology results of plate structures. (a) Case 1; (b) Case 2

[DOI: 10.22068/ijoce.2025.15.2.639]

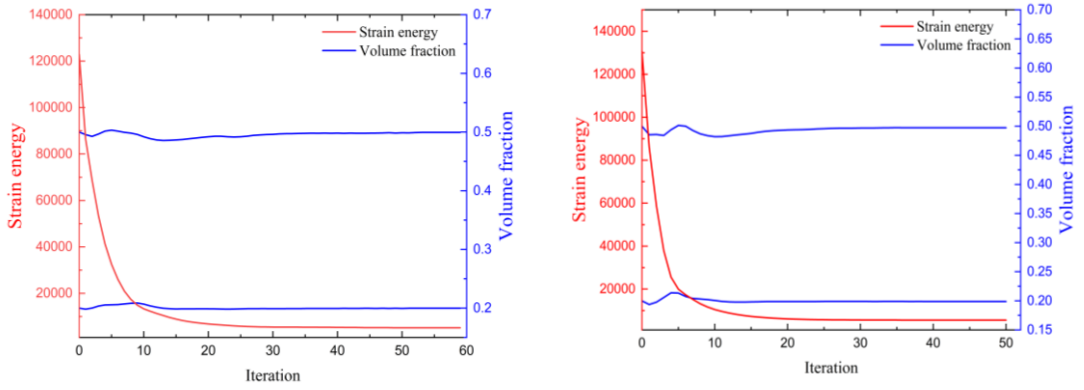

(a) (b)

Figure 10: History of objective function and volume fraction of plate structure. (a) Case 1; (b) Case 2

7.4. Example 4

Topology optimization of a shell structure is considered as the final example of this article. This example considers a shell structure with simply supported boundary condition at all four corners as depicted in Figure 11. The design domain is discretized by 50×53 quadratic finite elements. The external force F in Figure 11 is assumed to be 1000 kgf. Topology optimization of two materials are investigated in which modulus of elasticities for material 1 and material 2 are 2×10^6 kg/cm^2 and 2×10^4 kg/cm^2, respectively. The volume fraction that used in this example is listed in Table 4. The topology of the optimum solution and convergence history of the objective function and volume fractions are shown in Figures 12 and 13, respectively. The stiffer material forms the core of the structure, connecting the point load to the supports in the high-stress regions, while the more compliant material is distributed around this core.

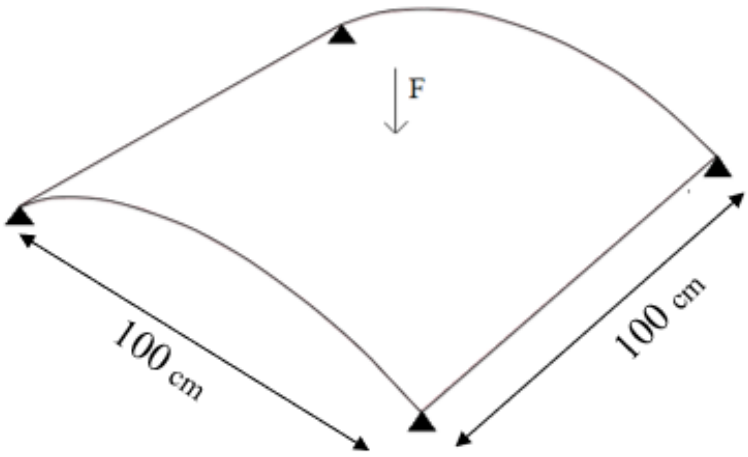

Figure 11. Geometry and boundary conditions

[DOI: 10.22068/ijoce.2025.15.2.639]

Table 4: Volume fraction constraint for the shell structure

Case no.	Total material $(\frac{V_{\text{total-max}}}{V_{\text{design space}}})\%$	Material 1 $(\frac{V_1}{V_{\text{design space}}})\%$	Material 2 $(\frac{V_{\text{total-max}}-V_1}{V_{\text{design space}}})\%$
1	50	20	30

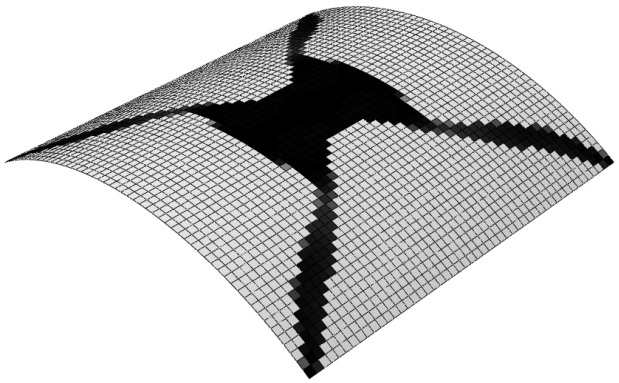

Distribution of material 1

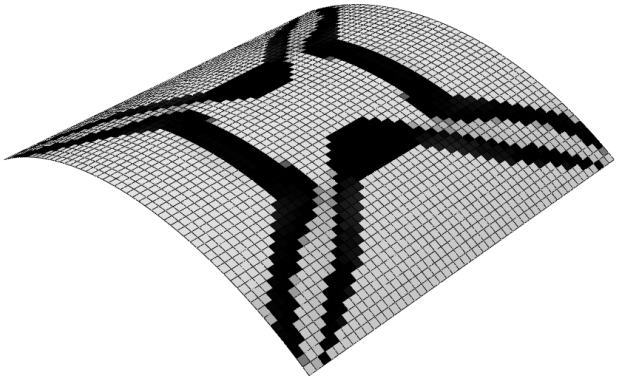

Distribution of material 2

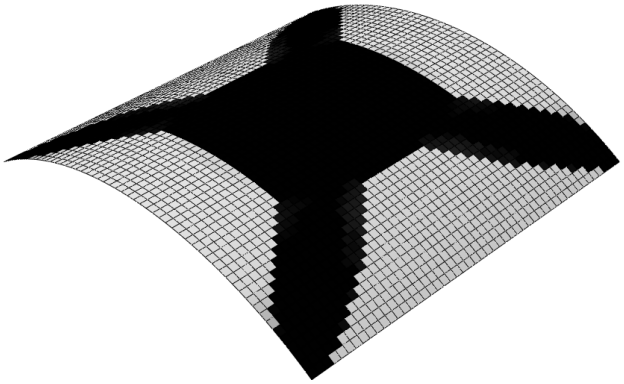

Distribution of both materials

Figure 12: Optimum topology results for the shell structure

[DOI: 10.22068/ijoce.2025.15.2.639]

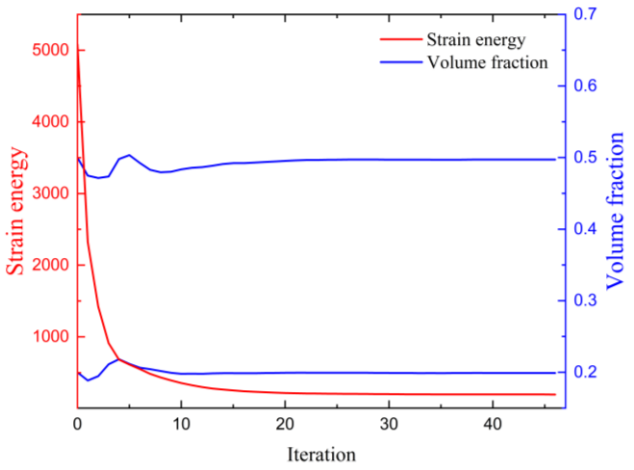

Figure 13: History of objective function and volume fraction of shell structure

8. CONCLUSION

In this study, multi-material topology optimization for plane, plate and shell structures is investigated. For a two-material problem, the proposed approach uses two design variables per element and applies two volume constraints to regulate the material distribution. Sensitivity analysis is performed using an analytical method to evaluate the effect of design variables on the objective function and constraints. The Solid Isotropic Material with Penalization (SIMP) method is adopted for parameterization, and the Method of Moving Asymptotes (MMA) is utilized to solve the topology optimization problem. The numerical results demonstrate that the proposed method can effectively determine the optimal distribution of two materials within the specified design domain with satisfactory precision.

DECLARATION OF COMPETING INTEREST

On behalf of all authors, the corresponding author states that there is no competing financial interests or personal relationships that could have appeared to influence the study reported in this paper.

FUNDING

This research did not receive any specific grant from funding agencies in the public, commercial, or not-for-profit sectors.

REFERENCES

1. Bendsøe MP, Kikuchi N. Generating optimal topologies in structural design using a homogenization method. *Comput Methods Appl Mech Eng*. 1988;**71**(2):197–224.
2. Michell AGM. LVIII. The limits of economy of material in frame-structures. *Philos Mag*. 1904;**8**(47):589–97.

[DOI: 10.22068/ijoce.2025.15.2.639]

3. Bendsøe MP. Optimal shape design as a material distribution problem. *Struct Optim*. 1989;**1**:193–202.
4. Rozvany GI, Zhou M, Birker T. Generalized shape optimization without homogenization. *Struct Optim*. 1992;**4**:250–52.
5. Rozvany GI. *Structural Design via Optimality Criteria*. Mech Elast Inelast Solids. 1989.
6. Tavakkoli S, Hassani B. Isogeometric topology optimization by using optimality criteria and implicit function. 2014.
7. Hassani B, Hinton E. *Homogenization and Structural Topology Optimization: Theory, Practice and Software*. Springer Sci Bus Media; 2012.
8. Xie YM, Steven GP. A simple evolutionary procedure for structural optimization. *Comput Struct*. 1993;**49**(5):885–96.
9. Khanzadi M, Tavakkoli SM. Optimal plastic design of frames using evolutionary structural optimization. *Int J Civ Eng*. 2011;**9**(3).
10. Querin OM, Steven GP, Xie YM. Evolutionary structural optimisation (ESO) using a bidirectional algorithm. *Eng Comput*. 1998;**15**(8):1031–48.
11. Allaire G, Jouve F, Toader AM. Structural optimization using sensitivity analysis and a level-set method. *J Comput Phys*. 2004;**194**(1):363–93.
12. Sethian JA, Wiegmann A. Structural boundary design via level set and immersed interface methods. *J Comput Phys*. 2000;**163**(2):489–528.
13. Wang MY, Wang X, Guo D. A level set method for structural topology optimization. *Comput Methods Appl Mech Eng*. 2003;**192**(1–2):227–46.
14. Jahangiry HA, et al. Isogeometric level set topology optimization for elastoplastic plane stress problems. *Int J Mech Mater Des*. 2021;**17**(4):947–67.
15. Jahangiry HA, Tavakkoli SM. An isogeometrical approach to structural level set topology optimization. *Comput Methods Appl Mech Eng*. 2017;**319**:240–57.
16. Jahangiry HA, et al. Isogeometric level set-based topology optimization for geometrically nonlinear plane stress problems. *Comput-Aided Des*. 2022;**151**:103358.
17. Aminzadeh M, Tavakkoli SM. A parameter space approach for isogeometrical level set topology optimization. *Int J Numer Methods Eng*. 2022;**123**(15):3485–506.
18. Kaveh A, et al. Structural topology optimization using ant colony methodology. *Eng Struct*. 2008;**30**(9):2559–65.
19. Kaveh A, Kalatjari V. Topology optimization of trusses using genetic algorithm, force method and graph theory. *Int J Numer Methods Eng*. 2003;**58**(5):771–91.
20. Kaveh A, Shahrouzi M. Simultaneous topology and size optimization of structures by genetic algorithm using minimal length chromosome. *Eng Comput*. 2006;**23**(6):644–74.
21. Kaveh A, Talatahari S. Geometry and topology optimization of geodesic domes using charged system search. *Struct Multidiscip Optim*. 2011;**43**:215–29.
22. Kaveh A, Zolghadr A. Topology optimization of trusses considering static and dynamic constraints using the CSS. *Appl Soft Comput*. 2013;**13**(5):2727–34.
23. Kaveh A, Mahdavi V. Colliding bodies optimization for size and topology optimization of truss structures. *Struct Eng Mech*. 2015;**53**(5):847–65.
24. Kaveh A, Rezaei M. Optimum topology design of geometrically nonlinear suspended domes using ECBO. *Struct Eng Mech*. 2015;**56**(4):667–94.
25. Kaveh A, Rezaei M. Topology and geometry optimization of single-layer domes utilizing CBO and ECBO. *Sci Iran*. 2016;**23**(2):535–47.

[DOI: 10.22068/ijoce.2025.15.2.639]

26. Kaveh A, Hosseini SM, Zaerreza A. Size, layout, and topology optimization of skeletal structures using plasma generation optimization. *Iran J Sci Technol Trans Civ Eng*. 2021;**45**(2):513–43.
27. Kaveh A, Mahdavi VR. Multi-objective colliding bodies optimization algorithm for design of trusses. *J Comput Des Eng*. 2019;**6**(1):49–59.
28. Svanberg K. The method of moving asymptotes—a new method for structural optimization. *Int J Numer Methods Eng*. 1987;**24**(2):359–73.
29. Hassani B, Tavakkoli SM, Ghasemnejad H. Simultaneous shape and topology optimization of shell structures. *Struct Multidiscip Optim*. 2013;**48**(1):221–33.
30. Li K, Ye W. Improving efficiency in structural optimization using RBFNN and MMA-Adam hybrid method. *Adv Eng Inf*. 2024;**62**:102869.
31. Ling Z, et al. Topology optimization of constrained layer damping on plates using Method of Moving Asymptote (MMA) approach. *Shock Vib*. 2011;**18**(1–2):221–44.
32. Tavakkoli S, Hassani B, Ghasemnejad H. Isogeometric topology optimization of structures by using MMA. *Int J Optim Civ Eng*. 2013;**3**(2):313–26.
33. Kazemi H, Tavakkoli S, Naderi R. Isogeometric topology optimization of structures considering weight minimization and local stress constraints. *Int J Optim Civ Eng*. 2016;**6**(2):303–17.
34. Bendsøe MP, Sigmund O. Material interpolation schemes in topology optimization. *Arch Appl Mech*. 1999;**69**:635–54.
35. Sigmund O, Torquato S. Composites with extremal thermal expansion coefficients. *Appl Phys Lett*. 1996;**69**(21):3203–05.
36. Zuo W, Saitou K. Multi-material topology optimization using ordered SIMP interpolation. *Struct Multidiscip Optim*. 2017;**55**:477–91.
37. Yun KS, Youn SK. Multi-material topology optimization of viscoelastically damped structures under time-dependent loading. *Finite Elem Anal Des*. 2017;**123**:9–18.
38. Li Y, et al. FloatArch: A cable-supported, unreinforced, and re-assemblable 3D-printed concrete structure designed using multi-material topology optimization. *Addit Manuf*. 2024;**81**:104012.
39. Zhang XS, Paulino GH, Ramos Jr AS. Multi-material topology optimization with multiple volume constraints: a general approach applied to ground structures with material nonlinearity. *Struct Multidiscip Optim*. 2018;**57**(1):161–82.
40. Li C, Kim IY. Multi-material topology optimization for automotive design problems. *Proc Inst Mech Eng D J Automob Eng*. 2018;**232**(14):1950–69.
41. Chandrasekhar A, Suresh K. Multi-material topology optimization using neural networks. *Comput-Aided Des*. 2021;**136**:103017.
42. Feng Y, Yamada T. An assemblable interlocking joint generation method for multi-material topology optimization using interfacial partial stress constraints and dimensional constraints. *Comput Methods Appl Mech Eng*. 2025;**433**:117475.
43. Jeong H, et al. An advanced physics-informed neural network-based framework for nonlinear and complex topology optimization. *Eng Struct*. 2025;**322**:119194.
44. Doan QH, et al. Multi-material structural topology optimization with decision making of stiffness design criteria. *Adv Eng Inf*. 2020;**45**:101098.
45. Yang L, et al. Layout design of thin-walled structures with lattices and stiffeners using multi-material topology optimization. *Chin J Aeronaut*.

[DOI: 10.22068/ijoce.2025.15.2.639]

46. Zhao T, et al. Strut-and-Tie Models Using Multi-Material and Multi-Volume Topology Optimization: Load Path Approach. *ACI Struct J*. 2023;**120**(6).
47. Li Y, et al. Practical application of multi-material topology optimization to performance-based architectural design of an iconic building. *Compos Struct*. 2023;**325**:117603.
48. Chu S, et al. Topology optimization of multi-material structures with graded interfaces. *Comput Methods Appl Mech Eng*. 2019;**346**:1096–117.
49. Banh TT, Lee D. Multi-material topology optimization design for continuum structures with crack patterns. *Compos Struct*. 2018;**186**:193–209.
50. Jahangiry HA, Gholhaki M, Sharbatdar M. Topology optimization of stiffened steel shear wall with located openings. *Iran Univ Sci Technol*. 2020;**10**(1):117–36.
51. Zhengtong H, et al. Multimaterial layout optimization of truss structures via an improved particle swarm optimization algorithm. *Comput Struct*. 2019;**222**:10–24.
52. Kaveh A, Seddighian M. Simultaneously multi-material layout and connectivity optimization of truss structures via an Enriched Firefly Algorithm. *Struct*. 2020.
53. Salmanpour P, et al. Multi-material optimal design of 3D transmission towers using black hole mechanics optimization: Real-size examples. *J Comput Des Eng*. 2024;**14**:609–28.

[DOI: 10.22068/ijoce.2025.15.2.639]